Enhanced Visibility of Colonic Neoplasms Using Formulaic Ratio Imaging of Native Fluorescence

Bhaskar Banerjee, MD,[1,2,3]* Nathaniel S. Rial, MD, PhD,[1] Timothy Renkoski, MS,[2] Logan R. Graves,[3] Sirandon A.H. Reid, BS,[4] Chengcheng Hu, PhD,[5] Vassiliki L. Tsikitis, MD,[4] Valentine Nfonsom, MD,[4] Judith Pugh, MD,[6] and Urs Utzinger, MD[2,3]

[1]*Department of Medicine, College of Medicine, University of Arizona, Tucson, Arizona 85724*
[2]*Department of Biomedical Engineering, College of Engineering, University of Arizona, Tucson, Arizona 85721*
[3]*College of Optical Sciences, University of Arizona, Tucson, Arizona 85721*
[4]*Department of Surgery, College of Medicine, University of Arizona, Tucson, Arizona 85724*
[5]*School of Public Health, College of Public Health, University of Arizona, Tucson, Arizona 85724*
[6]*Department of Pathology, College of Medicine, University of Arizona, Tucson, Arizona 85724*

Background and Objectives: Colonoscopy is the preferred method for colon cancer screening, but can miss polyps and flat neoplasms with low color contrast. The objective was to develop a new autofluorescence method that improves image contrast of colonic neoplasms.

Study Design/Materials and Methods: We selected the three strongest native fluorescence signals and developed a novel method where fluorescence images are processed in a ratiometric formula to represent the likely cellular and structural changes associated with neoplasia. Native fluorescence images of fresh surgical specimens of the colon containing normal mucosa, polypoid and flat adenomas as well as adenocarcinoma were recorded using a prototype multi-spectral imager. Sixteen patients, with a mean age of 62 years (range 28–81) undergoing elective resection for colonic neoplasms were enrolled. High contrast images were seen with fluorescence from tryptophan (Tryp), flavin adenine dinucleotide (FAD) and collagen.

Results: When the image intensity of Tryp was divided pixel by pixel, by the intensities of FAD and collagen, the resulting formulaic ratio (FR) images were of exceptionally high contrast. The FR images of adenomas and adenocarcinomas had increased Weber contrast.

Conclusions: FR imaging is a novel imaging process that represents the likely metabolic and structural changes in colonic neoplasia that produces images with remarkably high contrast. Lasers Surg. Med. 45:573–581, 2013.

Key words: colon; cancer; polyps; fluorescence; imaging

INTRODUCTION

Colonoscopy is the preferred method of screening for colorectal cancer but it has its shortcomings. It has a sensitivity of 90% for adenomatous lesions greater than 10 mm [1]. Tandem colonoscopies have shown that 22% of polyps can be missed and compared to virtual colonoscopy, it can miss up to 10% of sessile or pedunculated polyps [2]. The yield of colonoscopy is affected by the endoscopic technique and factors including time of day, queue position and quality of prep [3,4]. With endoscopists trying to maximize their productivity in terms of number of patients examined, the quality of examinations is at risk.

Colonoscopy is successful at detecting adenomatous polyp lesions, especially left-sided, with subsequent polypectomy and decreased CRC mortality [5]. The effectiveness of colonoscopy in the proximal colon has been questioned in some studies, as lesions can be missed [5,6]. . Serrated- and flat-lesions can escape detection by the unaided eye, due to a lack of color contrast compared to the surrounding mucosa [7]. Indeed the detection rate of proximal, serrated lesions varied widely in one recent report, from 0.01 to 0.26 [8]. Of some concern are the "interval" cancers lesions that are detected within a few years of screening, with devastating consequences for patients and care-givers alike [5]; although some may be due to accelerated transformation, a significant number are the result of lesions not being seen by the endoscopist [9].

Chromoendoscopy uses topical dyes to improve the visibility of lesions and hence their detection during endoscopy [7]. It can help unmask flat neoplasms, but the time requirements, learning curve and potential safety issues of some dyes makes it unlikely to be widely incorporated into practice [10]. The ideal solution would be a wide-field imaging technique that indicates the location of neoplasms, including those that are difficult to see with the naked eye, without the dependence of

Conflicts of Interest Disclosures:
Contract grant sponsor: National Institutes of Health; Contract grant number: R01CA098341; Contract grant sponsor: Marshall Foundation & Arizona Technology Research Initiative.
*Correspondence to: Bhaskar Banerjee, MD, Division of Gastroenterology, Room 6402, 1501 N. Campbell Avenue, PO Box 245028, Tucson, AZ 85724-5028.
E-mail: bbanerjee@deptofmed.arizona.edu
Accepted 8 September 2013
Published online 30 September 2013 in Wiley Online Library (wileyonlinelibrary.com).
DOI 10.1002/lsm.22186

exogenous chemicals. To pursue this, narrow band imaging (NBI, Olympus, Inc., New Hope, PA), which uses blue and green light that is avidly absorbed by hemoglobin and displays blood vessels with high contrast was introduced. This was followed by flexible spectral-Imaging Color enhancement (FICE, Fujinon, Inc., Wayne, NJ), which uses white light illumination followed by spectral estimation of the reflected light to produce high contrast images. However, neither NBI, FICE, nor i-scan (Pentax Medical Co, Montvale, NJ) have been shown to improve the detection rate of neoplasms compared to high resolution white light endoscopy [11,12].

Endoscopes using autofluorescence have also been developed to help improve neoplasm detection. A number of native fluorophores are present in tissues, most notably reduced nicotinamide adenine dinucleotide (NADH), flavin adenine dinucleotide (FAD), tryptophan, collagen, elastin, and porphyrins [13]. Initial work with fiberoptic instruments showed that broad band fluorescence decreases with neoplastic change, which led to the development of autofluorescence endoscopes [14]. Auto-fluorescence imaging (AFI) is an endoscopic autofluorescence system (Olympus, Inc.) where blue light excitation in the 400–500 nm wavelength range produces autofluorescence at 490–625 nm. A reflectance image of the mucosa is taken with green light (550 nm) and a pseudocolor (magenta) is computed to indicate areas of decreased fluorescence, with the surrounding normal mucosa appearing green from reflected light [15,16]. The Onco-Life (OL) system (Xillix Technologies Corporation, Richmond, BC, Canada) uses blue light (400–450 nm) for excitation, captures fluorescence from 490 to 560 nm and combines it with a red reflectance image [17]. The results from autofluorescence endoscopes have been mixed, with some showing increased detection of polyps, while others revealed no difference to white light endoscopy and missed detection of flat neoplasms [16,17].

The need is for a wide-field optical technique that sufficiently enhances the image contrast of low color contrast lesions, to facilitate their detection during a busy endoscopy schedule, even at the end of the queue.

Noting that prior use of autofluorescence endoscopy has been limited to visible fluorescence with unselected contributions from a number of fluorophores, we investigated fluorescence at shorter, ultra violet (UV) wavelengths and combined it with selected fluorescence signals to help increase the image contrast of neoplasms. The higher the contrast, the easier it should be to detect neoplasms.

Fluorescence images from tryptophan, NADH, FAD and collagen were studied. The amino acid Tryptophan is the predominant source of fluorescence in cells and when illuminated at 280 nm, the emission peak at 330–340 nm is significantly greater in cancerous cells compared to cells from the normal mucosa [18,19]. Further, the intensity of tryptophan fluorescence in dysplastic intestinal polyps has been correlated with increased tissue tryptophan content [18]. Similarly, the fluorescence from NADH (400–500 nm, with a peak at 450 nm) also increases in neoplastic change [20]. Conversely, fluorescence from FAD (400–600 nm, with a peak at 550 nm) decreases with malignant transformation due in part to the anaerobic metabolism of glucose [13,21,22]. Basement membrane collagen is the major fluorophore in the extracellular matrix; its observed fluorescence decreased in neoplasia due to its degradation by matrix metalloproteinases and its increased distance from the epithelial surface [13]. The native fluorescence from tryptophan, reduced NADH, FAD and collagen were explored, however the high contrast images were consistently associated with tryptophan, collagen and FAD fluorescence, with corresponding excitation wavelengths of 280, 320, and 440 nm (data not presented here). The three signals were therefore selected for formulaic imaging.

We hypothesized that the formulaic ratio (FR) image produced by the dividend of Tryp/(Collagen $\times$ FAD) fluorescence intensities would produce high contrast images of colonic neoplasms due to the inherent changes that accompany the neoplastic process.

MATERIALS AND METHODS

Spectral Imager

A prototype wide field Xenon-lamp based spectral imager capable of illumination from 260 to 650 nm and detection from 340 to 650 nm was used to measure tissue autofluorescence and reflectance. Details of the instrument have been published earlier; a representative diagram of the apparatus is shown in Figure 1 [23]. Specimens were illuminated from above with narrow bandpass interference filters, with full width at half maximum of approximately 20 nm. Longpass filters were mounted in a ten-position filter wheel below the CCD 16 bit camera. Details of the excitation, emission and reflectance wavelengths used for imaging and the target tissue constituents are given in Table 1. Images are named specifying fluorescence or reflectance wavelengths (F280, F370, F440, F440Red, and R555) where F corresponds to fluorescence and R represents reflectance. The 280-nm excited (predominantly Tryptophan) fluorescence image (F280) was formed by subtracting 410 nm longpass image from 300 nm longpass image (Table 1). Similarly, autofluorescence images from 370 nm excitation (Collagen, NADH & Elastin) were captured between 410 and 500 nm (F370) and images with 440 nm excitation (FAD & Collagen) were recorded between 500 and 600 nm (F440) [24]. R555 represents the diffuse reflectance image collected where 555 nm is the center of the narrow band illumination beam. Excitation at 370 nm leads to emission from both collagen and NADH; with neoplastic change, the emission from NADH is expected to increase and that from collagen to decrease, however, as has been shown in cervical tissue, the contribution from collagen to the emission in this wavelength range is greater than that of NADH [24].

Multi-Spectral Imaging and Image Processing

Fresh surgical specimens of the colon were studied from patients undergoing elective colectomy for neoplasms of

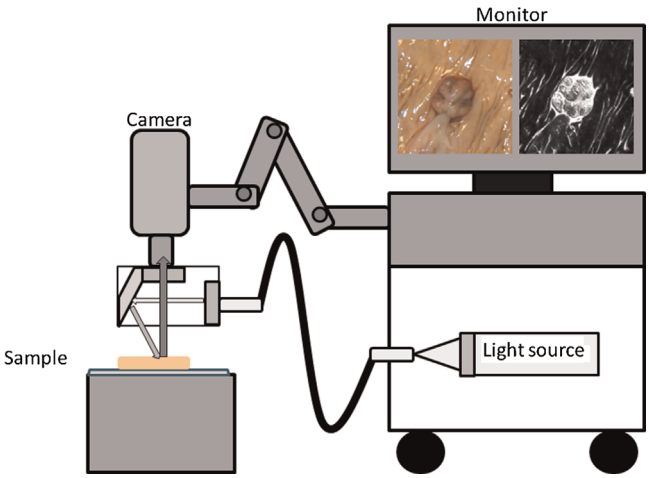

Fig. 1. The spectral imager consists of a mobile cart containing a computer, filter wheel controller, and a light source providing illumination from 260 nm to 650 nm through optical bandpass filters. A flexible fiberoptic cable guides the light towards the sample. To adjust the illuminated field the fiber output is collimated and reflected by a mirror towards the sample. Light emitted from the sample is collected through optical filters and imaged with an UV-objective onto a CCD camera (adapted from Banerjee et al. [23]).

the colon. Specimens of resected segments of colons (about 30 cm in length and 0.5 cm in thickness) were collected immediately after resection, transported to the imaging laboratory in a closed plastic container and irrigated with normal saline to remove stool and/or blood. Imaging took less than a minute to complete and was performed 30–45 minutes after resection at normal room temperature. Each specimen was rinsed and kept moist with normal saline and a color image of each lesion was taken with a digital camera (Nikon D100, Nikon, Inc., Melville, NY). The captured autofluorescence images were saved as 16 bit TIFF files and loaded into Matlab as 512×512 image files (Mathworks, Natick, MA) for production of ratio images. First images were corrected for power fluctuations of the light source, exposure time of the camera and spatial variation of illumination intensity. The light source power was measured continuously during imaging and the spatial illumination distribution was measured with a reflecting standard each day.

TABLE 2. Images Used to Compare FR With Sim A and Sim B

Imaging method	Formulae	Refs.
FR	$F280/(F370 \times F440)$	
Sim A	F440R/F440	[25]
Sim B	R555/F440	[26]

To create a formulaic ratio (FR), for example A/B, the intensity value associated with each individual pixel in image A was divided by the intensity value of the corresponding pixel in image B. If a ratio involved multiplication, the intensities were multiplied. The formulae used to create final images, including FR, are given Table 2. Ratio images were analyzed to determine an ideal high and low intensity value for display. The same values were then used to scale all displayed images produced by said ratio. For example, if FR images contained numbers in the range of 0.5–15 and the display allows levels between 0 and 255, the FR image was scaled so that 0.5 was represented with 0 and 15 with 255. When determining the range of intensities in the FR images, all samples were considered.

Weber contrast was measured to designate the difference in luminance that made a lesion distinguishable from its surrounding. Mathematically it is represented as: $(I-I_m)/I_m$, where I is the luminance of the lesion and I_m is the luminance of the surrounding mucosa. Regions of interest (ROI) were formed as outlined in our images by two of the investigators (N.S.R., L.R.G.), who received the color and Tryptophan associated images to draw the ROI around the lesion borders and a comparable area from the normal appearing mucosa. The average intensity within a region was representative for either the lesion or the surrounding mucosal intensity.

To compare the contrast of FR images to existing autofluorescence technologies, grayscale images were created approximating the color contrast of the pseudocolor images produced by two existing AF systems. Sim A is a ratio image formed by dividing F440R by F440 when excited by blue light at 440 nm. It simulates the red/green ratio reported by Zeng et al. [25] and used by the OL system to identify polyps. Sim B is an image formed by dividing R555 by F440 excited by blue light at 440 nm; it simulates

TABLE 1. Imaging Configurations and Their Association With Tissue Constituents (*F* = Fluorescence, *R* = Reflectance)

Image	Illumination (nm)	Emission (nm)	Target constituents	Other constituents
F280	280	300–410	Tryptophan	Pyridoxine
F370	370	410–500	Collagen	NADH, Elastin
F440	440	500–600	FAD	Collagen
F440 Red	440	600–680	Collagen	FAD
R555	540–570		Tissue Scattering	Hemoglobin absorption

the ratio described by Aihara et al. which is used to discriminate polyps in the AFI system [26]. Intensity differences in grayscale images Sim A and Sim B estimate the color differences realized by each colonoscope.

Informed consent was obtained from all patients prior to surgery, and the study was approved by the Institutional Review Board of the University of Arizona.

RESULTS

A total of 16 patients, six males and ten females with a median age of 63.5 years (range 28–81) undergoing elective resection for colonic neoplasms were enrolled Figure 2. There were four patients with distal adenocarcinomas, eight with proximal cancers (cecum to the splenic flexure), and four with neoplastic polyps. Of note, a single patient had four separate adenomatous polyps for a total of 19 lesions that were imaged for analysis.

Images representing adenocarcinomas are shown in Figure 3. Figure 3A shows a color image of a well differentiated adenocarcinoma of the sigmoid colon from a 64-year-old Native American woman, with F280, F370, F440 and the processed FR image in Figure 3B–E respectively. Compared to the surrounding mucosa, fluorescence is lower in the carcinoma in F280, markedly lower in the F370 image and higher in F440, whereas the FR image displays the lesions with high intensity and contrast and with little or no luminosity from the surrounding mucosa. A color photograph of a poorly differentiated adenocarcinoma of the ascending colon from a 68-year-old Caucasian woman is shown in Figure 3F, with F280, F370, F440 and the processed FR image presented in Figure 3G–K, respectively. The fluorescence of the cancer is comparable to the surrounding mucosa in F280, lower in F370 and F440, whereas the processed FR image displays it with high contrast, as an intensely bright lesion against a dark background.

Figure 4 shows images of adenomatous polyps from the colon of a 28-year-old Hispanic male with multiple polyps.

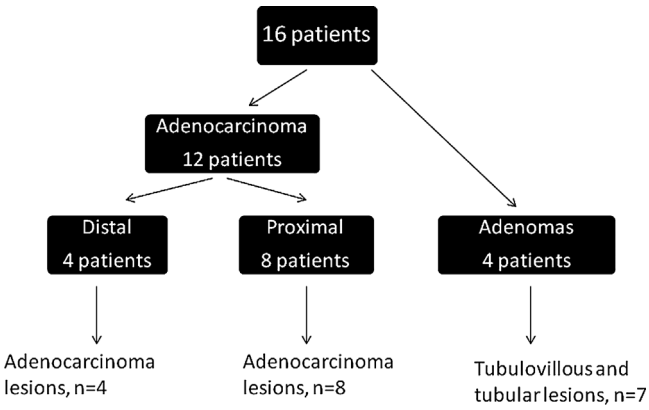

Fig. 2. A total of 16 patients were identified as having lesions from prior colonoscopy. Twelve had adenocarcinomas (four distal and eight proximal). Four patients had adenomas (one had four lesions, the rest had one each).

Compared to the color image of a 15 mm pedunculated polyp (Fig. 4A) the F280 image (Fig. 4B) shows slightly reduced fluorescence compared to the surrounding mucosa, however, the FR image (Fig. 4C) portrays the head but not the stalk with intense brightness against a dark mucosa. In Figure 4D, there appears to be a single, 3 mm, sessile lesion at the center of the color image. While the F280 image (Fig. 4E) shows this as an area of reduced fluorescence intensity, the FR image (Fig. 4F) displays not only the central polyp with high contrast, but an additional small area of brightness at the top of the image that was subsequently appreciated in the color image (Fig. 4D). Further inspection confirmed this to be another polyp. All lesions were adenomatous on histopathology.

Figure 5 illustrates the difference in contrast obtained by FR imaging compared to the simulated images of existing autofluorescence systems. The adenoma in Figure 4A was chosen as an example (color image not shown). Substantially higher contrast is seen in the FR image (Fig. 5D) than in simulated OL (Fig. 5E) or simulated AFI (Fig. 5F) images.

The mean Weber contrast for the FR images of adenocarcinomas was 5.07 ± 5.13, which was substantially greater than the corresponding mean Weber contrasts of Sim A and Sim B images of the same lesions: 0.22 ± 0.18 ($P = 0.0005$) and 0.21 ± 0.28 ($P = 0.008$) respectively, by Wilcoxon signed-rank test (Fig. 6A). The mean Weber contrast of FR images for adenocarcinomas was 5.07 ± 5.13 (Fig. 6A) which was about three times higher than the mean Weber contrast of adenomas, 1.51 ± 1.47 (Fig. 6B); the difference was marginally significant ($P = 0.10$; Wilcoxon rank-sum test). The FR images of adenomas (Fig. 6B) produced higher contrast than that of Sim A 0.18 ± 0.30 (marginally significant $P = 0.063$) and Sim B 0.11 ± 0.23 (not statistically significant $P = 0.25$) by Wilcoxon signed-rank test.

DISCUSSION

Our results show that formulaic ratio images of autofluorescence from tryptophan when divided by the fluorescence from collagen and FAD produce images with exceptional contrast that should improve polyp detection rates. By selectively using native fluorescence images in a formulaic ratio that represents the neoplastic process, we are able to generate images with exceptional contrast. Although ratio images have been used in the past, this work is unique in that it uses fluorescence images from three fluorophores and includes the use of UV wavelengths.

Raw tryptophan fluorescence images did not show neoplasms with high luminosity (Figs. 3 and 4), but the images are dramatically transformed when the tryptophan image was divided by the multiple of fluorescence from collagen and FAD (Figs. 3–5). The use of Weber contrast enables individual images to be directly compared to others. The FR images depicted adenocarcinomas with more than five times the intensity as the surrounding mucosa and adenomas with more than one and a half times the intensity of the mucosa. The divergence may be related

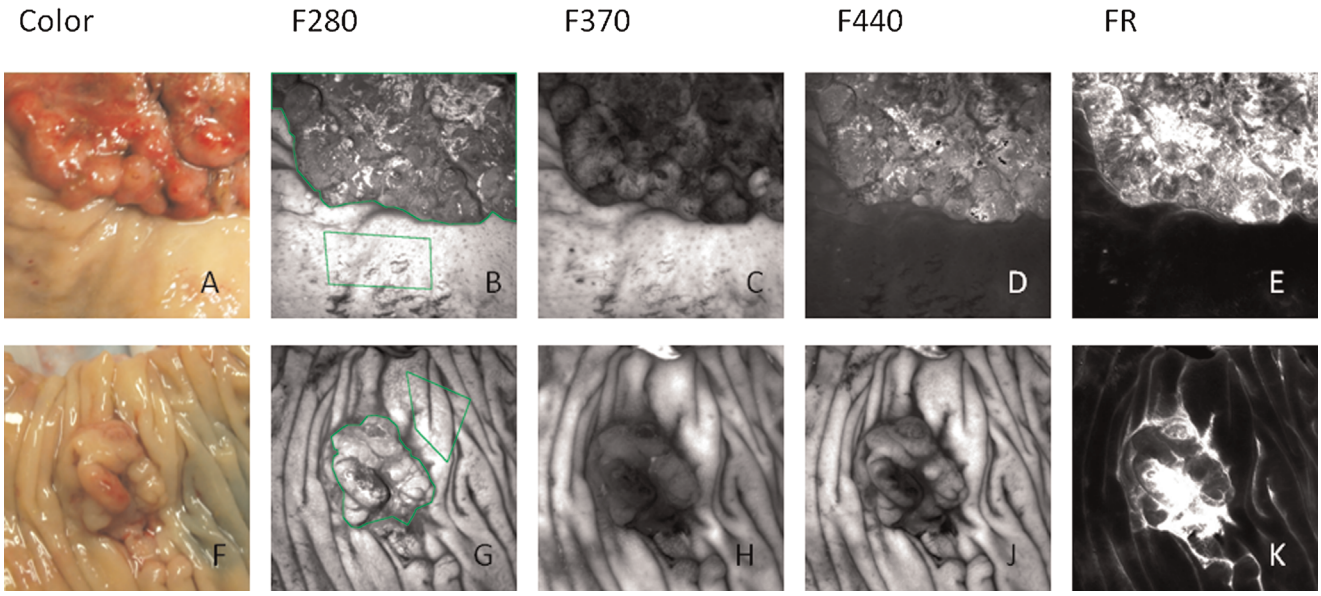

Fig. 3. Color image of surgical sample of a sigmoid colon adenocarcinoma (**A**), with grayscale images of F280 (**B**), F370 (**C**), F440 (**D**), and FR (**E**). A color image of an ascending colon adenocarcinoma is shown (**F**) followed by grayscale images of F280 (**G**), F370 (**H**), F440 (**J**), and FR image (**K**). Fluorescence images show lesions with similar or lower intensity than the surrounding mucosa, whereas the processed FR images display the same lesions with exceptional contrast. The borders of the areas used for calculating Weber contrast are indicated in green in (B) and (G).

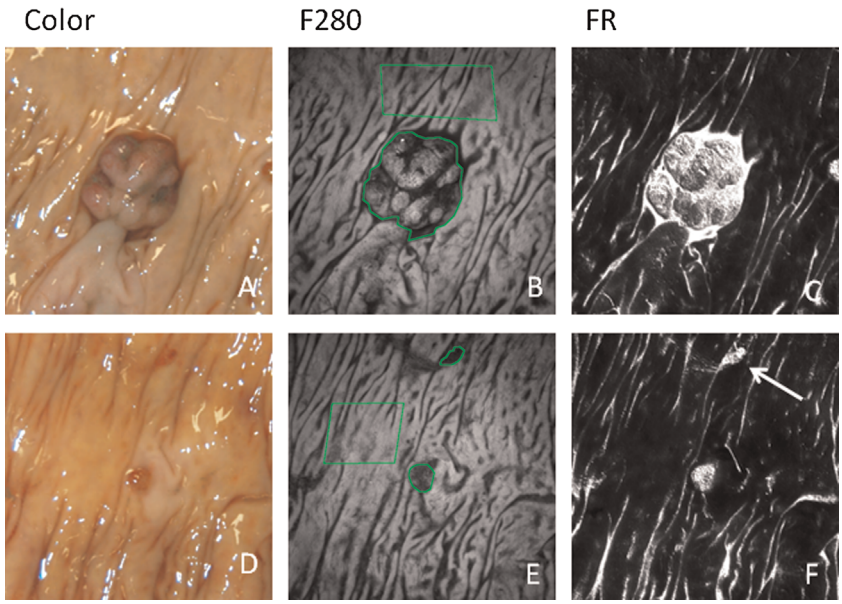

Fig. 4. Color image of a 15 mm pedunculated adenomatous polyp (**A**) is shown with grayscale images of F280 (**B**) and FR image (**C**). In the F280 image, the head of the polyp is shown with lower intensity than the surrounding mucosa, but the FR image displays the polyp head with intense contrast against a dark mucosal background. A 3 mm polyp is seen at the center of the color image (**D**), which is displayed with low contrast by the F280 image (**E**) but shown with very high contrast in the FR image (**F**). A small high contrast area (arrow) is recognized at the top of the image (F) which represents a smaller polyp that was not immediately noted in the color image (D). The borders of the areas used for calculating Weber contrast are indicated in green in (B) and (E).

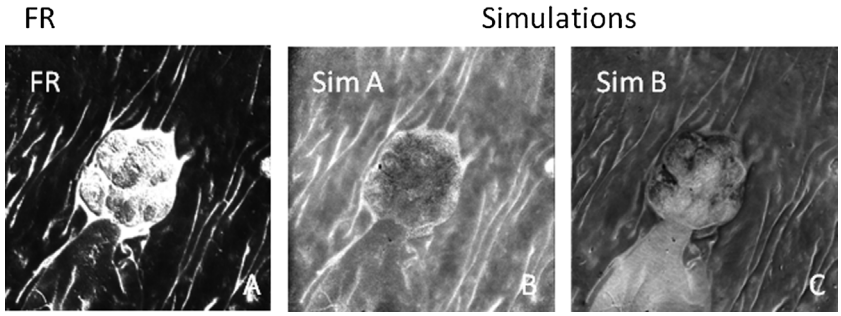

Fig. 5. Grayscale images of the 15 mm pedunculated adenomatous polyp from Figure 4A are shown as examples of relative contrast achieved with FR imaging (**A**), Sim A (**B**), and Sim B (**C**). FR imaging displays the polyp head but not the stalk with very high contrast and with higher contrast than Sim A and Sim B.

to the size and architectural differences between carcinomas and adenomas. Adenocarcinomas were larger, thicker and firmer in consistency than adenomas and are known to be more vascular, which would have affected fluorescence as well as scattering and absorption [27–29]. We believe these are the highest contrast images ever reported for a *label-free* imaging system in the gastrointestinal tract. Proximal colon neoplasms tend to be more aggressive, flatter in shape than distal lesions and have characteristic mutations [7,30]. A comparison of distal to proximal cancers revealed that the FR contrast for distal cancers were about three times greater than proximal colon cancers, but the difference was not significant and the data was thus not presented. However, this is consistent with the fact that proximal lesions are more difficult to detect during colonoscopy [5].

The image in Figure 4D was taken to capture the polyp at its center, however, bright fluorescence shown at the top of the FR image (Fig. 4F) caused a re-examination of the color image to recognize the presence of a much smaller adenomatous polyp that had been missed during the initial inspection. This illustrates the utility of this high contrast imaging system in capturing lesions that may escape the naked eye.

Tryptophan fluorescence was studied as it is the predominant source of fluorescence in cells, is more abundant in malignant cells than in normal cells of the same organ and its intensity was greater in dysplastic murine polyps compared to the normal mucosa [18]. However, raw tryptophan fluorescence images in the human colon displayed lesions with lower or comparable intensity to that of the surrounding mucosa. This is most likely due to a combination of altered scattering of light and increased absorption of the fluorescence by hemoglobin due to angiogenesis [31]. We have previously shown that the attenuated fluorescence from Tryptophan can be partly corrected when divided by a reflectance wavelength that is not readily absorbed by hemoglobin [23,32]. However, much higher contrast can be achieved when tryptophan fluorescence images are divided by fluorescence from FAD and collagen.

We believe this is a novel ratiometric use of three naturally fluorescent signals to display neoplasms with exceptional contrast in a "label-free" imaging system. Our technique is distinct from existing endoscopic autofluorescence systems as excitation and observation of the fluorescent signal from tryptophan occurs in the ultraviolet range, which is different from visible fluorescence used by the AFI and OL systems [15,33]. Furthermore, AFI and OL display both reflectance and fluorescence concurrently in separate color channels. The images in AFI and OL are dependent on unselected cellular and extracellular fluorophores of NADH, FAD, collagen and elastin as well as the effects of absorption and scattering, whereas our method restricts it largely to the three fluorophores that produce high contrast when used in a formulaic ratio [15,16]. The limitation of our work on surgical specimens is that it cannot be directly compared to an *in vivo* endoscopic study. However, Schoemaker has shown that *in vivo* results are often superior to *in vitro* [14]. Further, our own experience in measuring autofluorescence in ovarian tissue showed that *ex vivo* measurements can be reproduced *in vivo*, although the interruption of blood flow and the increased content of deoxyhemoglobin could affect the images [34,35]. By collecting fluorescence and reflectance data over a wide range of wavelengths, we were able to produce grayscale images that simulated the images produced by AFI and OL systems. Our FR images consistently produced greater contrast for cancerous lesions than that produced by Sim A and Sim B. The significantly greater contrast achieved with FR imaging compared to the simulated AFI and OL images is represented by the differences in mean contrast as depicted in Figure 6A,B. On average, FR images displayed adenomas with more than five times greater contrast than simulated AFI and OL images; adenocarcinomas with even higher contrast.

For adenomas (polypoid and flat), the magnitude of contrast achieved with FR imaging was superior to simulations of existing techniques, but the differences were not significant due to the small number of patients with adenomas, which are uncommon in surgical samples. We chose to image four polyps in a single patient as adenomatous lesions are infrequently encountered in surgical specimens, however the nonparametric Wilcoxon signed-rank test was used to account for this. Figure 4D–F shows how the system has the potential to detect small

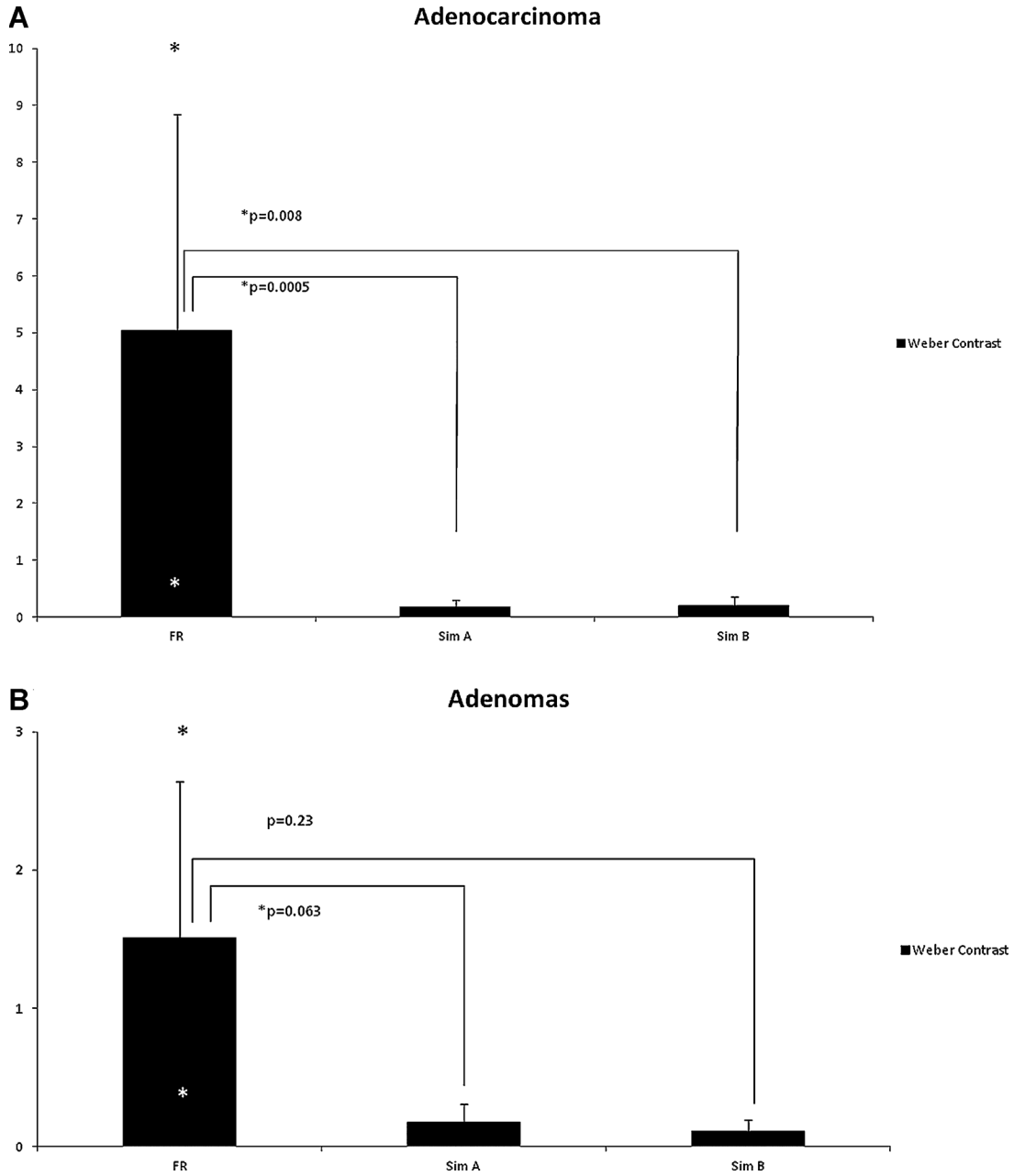

Fig. 6. **A**: The mean Weber contrast of all adenocarcinomas for the FR images was 5.07 ± 5.13. The * represent the 90th (10.1) and 10th (0.6) percentiles. For comparison, the mean Weber contrast $\pm$ SD for Sim A and Sim B images are provided. The Weber contrast of FR images was significantly superior to Sim A ($P = 0.0005$) and Sim B ($P = 0.008$) of the same images, by Wilcoxon signed-rank test. **B**: The mean Weber contrast of adenomatous lesions for the FR images was 1.51 ± 1.47. The * represent the 90th (3.0) and 10th (0.3) percentiles. The mean Weber contrast $\pm$ SD for Sim A and Sim B images are provided for comparison. The FR images produced higher contrast than Sim A, 0.18 ± 0.30 ($P = 0.063$) and Sim B, 0.11 ± 0.23 ($P = 0.25$) of the same images, by Wilcoxon signed-rank test.

lesions that can be missed on color images. Representative images in Figure 4A–F illustrate the remarkably high contrast achieved with FR, and in particular how the adenomatous head of the polyp was displayed with greater luminosity than the stalk.

We recognize that our comparison of different techniques involves a simple approximation of the existing systems, using grayscale mode, to allow easier comparison. Color included in commercialized imaging systems is based on earlier work that used grayscale imaging. We have

made comparisons to pseudocolor images in our prior work but chose to use grayscale images of AFI and OL to enable us to numerically compare contrast [36]. Finally, AFI and OL both exist as clinical in-vivo instruments, whereas FR remains to be developed into an endoscopic system.

Hyperplastic lesions were not reported in this study as they are uncommon in surgical specimens. However, our ongoing work involving non-surgical specimens has indicated that compared to adenomas and adenocarcinomas, hyperplastic polyps are displayed with little or no appreciable contrast in FR images. Compared to cancers, the availability of polyps from surgical specimens is limited, however our data indicates the potential of our technique in generating images with very high contrast.

Recently, Imaizumi et al. [37] reported a new fluorescence imaging technique including excitation at 365 nm (UV) and 405 nm (violet/blue) with observation in the blue. A ratio is formed by dividing images at those two excitation wavelengths while keeping the observation range constant. Their reported contrast ratios for tubular adenomas and hyperplastic polyps were lower than the contrast produced by FR imaging, however the relative contrast variation was similar. They reported that blood volume is unlikely to be a mechanism for their observed contrast.

The short-wavelengths required in the FR images have the potential to alter DNA. Although the direct effects of UV light on the intestinal mucosa are not known, there may be a risk for UV photo-toxicity [38]. We have previously shown that 280 nm illumination required for tryptophan fluorescence is limited to a penetration depth of approximately 100 microns into the colonic epithelium [23]. By contrast, the progenitor stem cells that are responsible for the proliferation of the colonocytes lay closer to the base of the crypts, approximately 500 microns below the luminal surface (about 50 cells deep) and therefore away from the potentially damaging wavelengths [39]. This is significant as the stem cells at the base of crypts produce colonocytes that migrate towards the luminal surface and the cells that would absorb any UV wavelengths, however briefly, would be shed and form a part of the stool [40,41]. We compared our imager to a hypothetical endoscope with a larger numerical aperture and reduced camera sensitivity and concluded that the light efficiency of the two would be comparable (data not presented). For instance, at 340 nm, we exposed tissue with about 2 Joules/m^2, and should be able to continuously image at that wavelength for several minutes while remaining approximately 100 times below the permissible UV exposure threshold for skin [42]. As the permissible UV threshold at 280 nm is about 3,000 times lower, imaging at this excitation wavelength would be safe, if limited to short video sequences of several seconds (as opposed to minutes), which should be sufficient to detect and localize a lesion [42]. Nevertheless, the safety of short wavelength illumination in the colon will need to be demonstrated using appropriate *in vivo* studies prior to use in patients [43,44].

The short wavelengths used by this technique require the use of special UV optics as transmission via standard optical materials is limited to wavelengths longer than 380 nm. Current efforts are underway to build such a device.

This is an exploratory investigation of using three autofluorescence signals used selectively in a formulaic ratio that represents the metabolic and structural changes of the neoplastic process, which produced images of very high contrast. The FR imaging system can be built into endoscopes to provide simultaneous side-by-side images to white light endoscopy and in-vivo validation in patients. Ultimately, the efficacy of the FR system will have to be evaluated in-vivo clinical trials once an endoscopic system is built. Such a system may lead to increased detection of neoplasms, particularly in the proximal colon, for which there is a clear need [45,46].

ACKNOWLEDGMENTS

This work was funded by grant R01CA098341 from the National Institutes of Health (U.U.), and the Marshall Foundation & the Arizona Technology Research Initiative Fund imaging fellowship (T.R.).

REFERENCES

1. Rockey DC, Paulson E, Niedzwiecki D, Davis W, Bosworth HB, Sanders L, Yee J, Henderson J, Hatten P, Burdick S, Sanyal A, Rubin DT, Sterling M, Akerkar G, Bhutani MS, Binmoeller K, Garvie J, Bini EJ, McQuaid K, Foster WL, Thomson WM, Dachman A, Halvorsen R. Analysis of air contrast barium enema, computed tomographic colonography, and colonoscopy: Prospective comparison. Lancet 2005; 365(9456):305–311.
2. van Rijn JC, Reitsma JB, Stoker J, Bossuyt PM, van Deventer SJ, Dekker E. Polyp miss rate determined by tandem colonoscopy: A systematic review. Am J Gastroenterol 2006; 101(2):343–350.
3. Gurudu SR, Ratuapli SK, Leighton JA, Heigh RI, Crowell MD. Adenoma detection rate is not influenced by the timing of colonoscopy when performed in half-day blocks. Am J Gastroenterol 2011;106(8):1466–1471.
4. Froehlich F, Wietlisbach V, Gonvers JJ, Burnand B, Vader JP. Impact of colonic cleansing on quality and diagnostic yield of colonoscopy: The European Panel of Appropriateness of Gastrointestinal Endoscopy European multicenter study. Gastrointest Endosc 2005;61(3):378–384.
5. Baxter NN, Goldwasser MA, Paszat LF, Saskin R, Urbach DR, Rabeneck L. Association of colonoscopy and death from colorectal cancer. Ann Intern Med 2009;150(1):1–8.
6. Brenner H, Hoffmeister M, Arndt V, Stegmaier C, Altenhofen L, Haug U. Protection from right- and left-sided colorectal neoplasms after colonoscopy: Population-based study. J Natl Cancer Inst 2010;102(2):89–95.
7. Soetikno RM, Kaltenbach T, Rouse RV, et al. Prevalence of nonpolypoid (flat and depressed) colorectal neoplasms in asymptomatic and symptomatic adults. JAMA 2008;299(9): 1027–1035.
8. Kahi CJ, Hewett DG, Norton DL, Eckert GJ, Rex DK. Prevalence and variable detection of proximal colon serrated polyps during screening colonoscopy. Clin Gastroenterol Hepatol 2011;9(1):42–46.
9. Rex DK. Maximizing detection of adenomas and cancers during colonoscopy. Am J Gastroenterol 2006;101(12):2866–2877.
10. Davies J, Burke D, Olliver JR, Hardie LJ, Wild CP, Routledge MN. Methylene blue but not indigo carmine causes DNA damage to colonocytes in vitro and in vivo at concentrations used in clinical chromoendoscopy. Gut 2007;56(1):155–156.

11. Rex DK, Helbig CC. High yields of small and flat adenomas with high-definition colonoscopes using either white light or narrow band imaging. Gastroenterology 2007;133(1):42–47.
12. Adler A, Aschenbeck J, Yenerim T, et al. Narrow-band versus white-light high definition television endoscopic imaging for screening colonoscopy: A prospective randomized trial. Gastroenterology 2009;136(2):410–416, e411; quiz 715.
13. Ramanujam N. Fluorescence spectroscopy of neoplastic and non-neoplastic tissues. Neoplasia 2000;2(1–2):89–117.
14. Schomacker KT, Frisoli JK, Compton CC, et al. Ultraviolet laser-induced fluorescence of colonic tissue: Basic biology and diagnostic potential. Lasers Surg Med 1992;12(1): 63–78.
15. Nakaniwa NNA, Ogihara T, Ohkawa A, Abe S, Nagahara A, Kobayashi O, Sasakki J, Sato N. Newly developed autofluorescence imaging videoscope system for the detection of colonic neoplasms. Digest Endosc 2005;17(3):235–240.
16. Uedo NHK, Ishihara R, Takeuchi Y, Iishi H. Diagnosis of colonic adenomas by new autofluorescence imaging system: A pilot study. Digest Endosc 2007;19:S134–S138.
17. Ramsoekh D, Haringsma J, Poley JW, et al. A back-to-back comparison of white light video endoscopy with autofluorescence endoscopy for adenoma detection in high-risk subjects. Gut 2010;59(6):785–793.
18. Banerjee B, Henderson JO, Chaney TC, Davidson NO. Detection of murine intestinal adenomas using targeted molecular autofluorescence. Dig Dis Sci 2004;49(1):54–59.
19. Kirkpatrick ND, Zou C, Brewer MA, Brands WR, Drezek RA, Utzinger U. Endogenous fluorescence spectroscopy of cell suspensions for chemopreventive drug monitoring. Photochem Photobiol 2005;81(1):125–134.
20. Chance B, Cohen P, Jobsis F, Schoener B. Intracellular oxidation-reduction states in vivo. Science 1962;137(3529): 499–508.
21. Pavlova I, Sokolov K, Drezek R, Malpica A, Follen M, Richards-Kortum R. Microanatomical and biochemical origins of normal and precancerous cervical autofluorescence using laser-scanning fluorescence confocal microscopy. Photochem Photobiol 2003;77(5):550–555.
22. Aboobaker VS, Bhattacharya RK. Modulation of flavocoenzyme levels in rat tissues by N-nitrosodiethylamine. Cancer Lett 1989;44(3):167–171.
23. Banerjee B, Renkoski T, Graves LR, et al. Tryptophan autofluorescence imaging of neoplasms of the human colon. J Biomed Opt 2012;17(1):016003.
24. Drezek R, Sokolov K, Utzinger U, et al. Understanding the contributions of NADH and collagen to cervical tissue fluorescence spectra: Modeling, measurements, and implications. J Biomed Opt 2001;6(4):385–396.
25. Zeng H, Weiss A, Cline R, MacAulay CE. Real-time endoscopic fluorescence imaging for early cancer detection in the gastrointestinal tract. Bioimaging 1998;6(4):151–165.
26. Aihara H, Sumiyama K, Saito S, Tajiri H, Ikegami M. Numerical analysis of the autofluorescence intensity of neoplastic and non-neoplastic colorectal lesions by using a novel videoendoscopy system. Gastrointest Endosc 2009; 69(3 Pt 2):726–733.
27. Kondo Y, Arii S, Mori A, Furutani M, Chiba T, Imamura M. Enhancement of angiogenesis, tumor growth, and metastasis by transfection of vascular endothelial growth factor into LoVo human colon cancer cell line. Clin Cancer Res 2000; 6(2):622–630.
28. St Croix B, Rago C, Velculescu V, et al. Genes expressed in human tumor endothelium. Science 2000;289(5482):1197–1202.
29. Faber DJ, Mik EG, Aalders MC, van Leeuwen TG. Light absorption of (oxy-)hemoglobin assessed by spectroscopic optical coherence tomography. Opt Lett 2003;28(16):1436–1438.
30. Hiraoka S, Kato J, Tatsukawa M, et al. Laterally spreading type of colorectal adenoma exhibits a unique methylation phenotype and K-ras mutations. Gastroenterology 2006; 131(2):379–389.
31. Zijlstra WG, Buursma A, Meeuwsen-van der Roest WP. Absorption spectra of human fetal and adult oxyhemoglobin, de-oxyhemoglobin, carboxyhemoglobin, and methemoglobin. Clin Chem 1991;37(9):1633–1638.
32. Bradley RS, Thorniley MS. A review of attenuation correction techniques for tissue fluorescence. J R Soc Interface 2006; 3(6):1–13.
33. Uedo N, Iishi H, Tatsuta M, et al. A novel videoendoscopy system by using autofluorescence and reflectance imaging for diagnosis of esophagogastric cancers. Gastrointest Endosc 2005;62(4):521–528.
34. George R. Early ovarian cancer detection using fluorescence spectroscopy in the ultraviolet-C through visible [Dissertation]. Tucson, AZ: Optical Sciences, University of Arizona; 2013.
35. George R, Michaelides M, Brewer MA, Utzinger U. Parallel factor analysis of ovarian autofluorescence as a cancer diagnostic. Lasers Surg Med 2012;44(4):282–295.
36. Renkoski T, Banerjee B, Graves LR, et al. Novel ratiometric imaging techniques and 280-nm excited autofluorescence for improved visualization of adenocarcinoma in human colon specimens. J Biomedical Optics 2013;18(1):016005; 016001–016011.
37. Imaizumi K, Harada Y, Wakabayashi N, et al. Dual-wavelength excitation of mucosal autofluorescence for precise detection of diminutive colonic adenomas. Gastrointest Endosc 2012;75(1):110–117.
38. Matthes RMA, Bernhardt JH, Ahlbom A, Cesarini JP, de Gruijl FR, Hietanen M, Owen R, Sliney DH, Soderberg P, Swerdlow AJ, Taki M, Tenforde TS, Vecchia B, Veyret B, Repacholi MH, Diffey B, Mainster MA, Okuno T, Stuck BE, Radiati ICN. Guidelines on limits of exposure to ultraviolet dariation of wavelengths between 180 nm and 400 nm (incoherent optical radiation). Health Phys 2004;87(2):171–186.
39. McTiernan A, Yasui Y, Sorensen B, et al. Effect of a 12-month exercise intervention on patterns of cellular proliferation in colonic crypts: A randomized controlled trial. Cancer Epidemiol Biomarkers Prev 2006;15(9):1588–1597.
40. Marshman E, Booth C, Potten CS. The intestinal epithelial stem cell. BioEssays 2002;24(1):91–98.
41. Tsubouchi S, Leblond CP. Migration and turnover of enteroendocrine and caveolated cells in the epithelium of the descending colon, as shown by radioautography after continuous infusion of 3H-thymidine into mice. Am J Anat 1979; 156(4):431–451.
42. Matthes R, McKinlay AF, Bernhardt JH, et al. Guidelines on limits of exposure to ultraviolet radiation of wavelengths between 180 nm and 400 nm (incoherent optical radiation). Health Phys 2004;87(2):171–186.
43. Heddle JA, Dean S, Nohmi T, et al. In vivo transgenic mutation assays. Environ Mol Mutagen 2000;35(3):253–259.
44. Heddle JA, Martus HJ, Douglas GR. Treatment and sampling protocols for transgenic mutation assays. Environ Mol Mutagen 2003;41(1):1–6.
45. Singh H, Nugent Z, Demers AA, Kliewer EV, Mahmud SM, Bernstein CN. The reduction in colorectal cancer mortality after colonoscopy varies by site of the cancer. Gastroenterology 2010;139(4):1128–1137.
46. Iacopetta B. Are there two sides to colorectal cancer? Int J Cancer 2002;101(5):403–408.